JOURNAL OF GUIDANCE, CONTROL, AND DYNAMICS
Vol. 24, No. 4, July–August 2001

Computational Aspects of Transfer Trajectories to Halo Orbits

Jean Albert Kechichian*
The Aerospace Corporation, El Segundo, California 90245-4691

The method of regularization is applied to the singular differential equations of the restricted circular three-body model in rotating coordinates centered at the L_1 Lagrange libration point of the sun–Earth system. The regularized equations are used through an iterative process to generate converged transfer trajectories from a low circular parking orbit around the Earth to the vicinity of the L_1 point, where a small velocity change inserts the spacecraft into a desired periodic halo orbit. These computation methods, which use backward numerical integration to provide a transfer solution that meets the end or boundary conditions with 1-m accuracy, are based on the use of double precision integrators with built-in interpolators as well as an unconstrained optimization algorithm that minimizes the summed squares of the differences between certain achieved parameters and their desired target values. The existence of optimal values of certain target parameters that lead to the minimization of the velocity change needed to insert into the halo orbit of interest is also shown, as well as the range of its feasible values at least in the case of the perigee location of the departure hyperbola.

Introduction

THE computation of the halo orbits and their transfer paths from the Earth has been pioneered by Farquhar,[1] Farquhar et al.[2,3] and Farquhar,[4] and various aspects of the trajectories and orbital maneuvers carried out by the International Sun-Earth Explorer-3 (ISEE-3) have been thoroughly discussed by the same authors. Much of the analyses and preliminary mission studies carried out to date have used the restricted circular three-body model in rotating coordinates adequately describing the motion of a vehicle moving in space and subject to the attraction of a binary system. These equations of motion, valid for any two primaries, are readily specialized to the sun–Earth system by properly accounting for its geometric and mass distribution characteristics. However, the differential equations in terms of the rotating coordinates have singularities when the distance to the massive bodies becomes very small, and this introduces truncation and roundoff errors during the numerical integration at closest approach. To avoid these errors during integration, the original differential equations are regularized[5,6] following the well-established procedure introduced by Kustaanheimo,[7] Kustaanheimo and Stiefel,[8] Levi-Civita,[9] and Stiefel and Scheifele.[10] This procedure removes the singularity near one of the massive bodies, in this case the Earth. It transforms the three second-order differential equations for the state vector components into a system of four second-order equations in the new parameters, and the physical time becomes a coordinatelike variable that is integrated with respect to a timelike independent variable. The regularized equations were used in Refs. 5 and 6, and in particular in Ref. 6, to solve the Earth-to-L_1 transfer problem in a barycentric rotating system. It was then apparent that the search must be conducted backward starting from the vicinity of the L_1 point because the trajectory is very sensitive to small changes in the state vector, especially its velocity components near the Earth, such that a forward integration of the regularized equations quickly diverges from a path that would lead the spacecraft to the vicinity of the Lagrange point. The trajectory being less sensitive to small perturbations to the state vector near the libration point, a successful iterative procedure that converges on a desired transfer path that meets the end boundary conditions is essentially feasible only with the backward integration scheme. Because the integration is computed with respect to a timelike variable, it is not possible to terminate a trajectory at a desired final time unless the integrator has a builtin interpolator that allows it to do so.

The next sections show the main elements of the theory of regularization of singular differential equations central to the successful development of robust software for transfer trajectory generation[10] as well as the equations of motion in terms of rotating coordinates centered at the sun–Earth barycenter.[5,6] The subsequent section develops the regularized system in terms of rotating coordinates centered at the more convenient location of the L_1 point. Several simulation methods are described, starting from the simpler one that uses the original singular system[1] and the Newton–Raphson solvers (see Ref. 11), with the physical time as the independent variable, to the more sophisticated method that uses the regularized variables corresponding to the L_1-centered rotating coordinates as well as an unconstrained optimizer and a double precision integrator with builtin interpolator.[12] In a first step, only the in-plane components of the small velocity change at a particular location on the halo orbit are searched on, in order to match a desired altitude above Earth, as well as a desired argument of perigee that will locate the place where the injection velocity change must be applied on the original circular parking orbit. Both the inclination and the node of the departure or injection orbit at low Earth orbit (LEO) are left uncontrolled in this scheme, which also shows that there exists a range of values for the argument of perigee for which such a transfer can be found and is feasible. The termination criterion of each backward integration trajectory during the iterative process is chosen as the dot product of the radius and velocity vectors at the perigee point, and this product is driven to zero by the interpolator triggering thereby the termination of the numerical integration. The transfer time is a byproduct of the converged search, and because it is not known a priori, a further iteration is carried out so that the backward integration also terminates at time zero; otherwise, the position of the Earth in its orbit around the sun will not be the exact one at the start of the integrations. This two-parameter search is next extended to the full three-parameter search whereby all three velocity vector components at the halo orbit location are searched on to match a desired altitude, argument of perigee, and inclination at the LEO injection point. These robust software codes provide converged transfer trajectories with meter accuracy, as is shown by several examples. It is also shown that there exists an optimal value of the target argument of perigee for a given target altitude, which minimizes the insertion cost. The analysis presented here also can be extended to the full and more accurate restricted elliptic problem for more exacting solutions.

Regularization of Singular Differential Equations

The main elements of the techniques of regularization[10] of singular differential equations are shown in this section for the sake of completeness. The Kustaanheimo–Stiefel mapping[8] transforms the original differential equations of the restricted circular three-body problem in terms of rotating Cartesian coordinates into a set of

Received 4 January 2000; revision received 9 October 2000; accepted for publication 17 November 2000.

*Engineering Specialist, P.O. Box 92957, Astrodynamics Department, MS M4/947, Los Angeles, CA 90009; Jean.A.Kechichian@aero.org. Associate Fellow AIAA.

differential equations in new parameters together with a change in the independent variable. The first step of regularization consists of introducing a new independent variable s such that, in the trivial one-dimensional case, the velocity with respect to s is $x\dot{x}$ and $\mathrm{d}x/\mathrm{d}s = x(\mathrm{d}x/\mathrm{d}t)$. This fictitious time s is defined by

$$\frac{\mathrm{d}}{\mathrm{d}s} = x\frac{\mathrm{d}}{\mathrm{d}t}, \qquad \mathrm{d}t = x\,\mathrm{d}s, \qquad t = \int x\,\mathrm{d}s$$

The transformation from ordinary to fictitious time is carried out by

$$\frac{\mathrm{d}}{\mathrm{d}t} = \frac{1}{x}\frac{\mathrm{d}}{\mathrm{d}s}$$

$$\frac{\mathrm{d}^2}{\mathrm{d}t^2} = \frac{\mathrm{d}}{\mathrm{d}t}\left(\frac{1}{x}\frac{\mathrm{d}}{\mathrm{d}s}\right) = \frac{1}{x}\frac{\mathrm{d}}{\mathrm{d}s}\left(\frac{1}{x}\frac{\mathrm{d}}{\mathrm{d}s}\right) = \left(x\frac{\mathrm{d}^2}{\mathrm{d}s^2} - \frac{\mathrm{d}x}{\mathrm{d}s}\frac{\mathrm{d}}{\mathrm{d}s}\right)\Big/x^3$$

Thus, the coordinate x and the physical time t are expressed in terms of the parameter s by way of this technique of uniformization. The second step of regularization consists of letting $x = u^2$. Given $x(0)$ and $\dot{x}(0)$ at $t = 0$, these transformations provide $u(0)$ and $u'(0)$ at $s = 0$. The regularization in two dimensions amounts to the squaring technique of Levi-Civita,[9] namely, $x_1 + ix_2 = (u_1 + iu_2)^2$. This transformation relates the coordinates x_1 and x_2 to the parameters u_1 and u_2 with $\boldsymbol{u} = (u_1, u_2)$ being the position vector of the particle in the (u_1, u_2) parametric plane. Thus, $x_1 = u_1^2 - u_2^2$, $x_2 = 2u_1u_2$, and

$$\begin{pmatrix} x_1 \\ x_2 \end{pmatrix} = L(\boldsymbol{u})\begin{pmatrix} u_1 \\ u_2 \end{pmatrix} \tag{1}$$

$$\begin{pmatrix} x_1' \\ x_2' \end{pmatrix} = 2L(\boldsymbol{u})\begin{pmatrix} u_1' \\ u_2' \end{pmatrix} \tag{2}$$

or in compact form, $\boldsymbol{x} = L(\boldsymbol{u})\boldsymbol{u}$ and $\boldsymbol{x}' = 2L(\boldsymbol{u})\boldsymbol{u}'$. The solution of $\boldsymbol{u}'$ in terms of $\boldsymbol{x}'$ is given by[10]

$$\boldsymbol{u}' = (1/2r)L^T(\boldsymbol{u})\boldsymbol{x}' = (1/2|\boldsymbol{u}|^2)L^T(\boldsymbol{u})\boldsymbol{x}' \tag{3}$$

It can also be shown by inspection that $L'(\boldsymbol{u}) = L(\boldsymbol{u}')$ and for any two vectors $\boldsymbol{u}$ and $\boldsymbol{v}$ that $L(\boldsymbol{u})\boldsymbol{v} = L(\boldsymbol{v})\boldsymbol{u}$. In three dimensions, Kustaanheimo[7] and Kustaanheimo and Stiefel[8] (KS) generalized the $L(\boldsymbol{u})$ matrix of Levi-Civita[9] using the four vector $\boldsymbol{u}$,

$$L(\boldsymbol{u}) = \begin{pmatrix} u_1 & -u_2 & -u_3 & u_4 \\ u_2 & u_1 & -u_4 & -u_3 \\ u_3 & u_4 & u_1 & u_2 \\ u_4 & -u_3 & u_2 & -u_1 \end{pmatrix}$$

If a three-vector $\boldsymbol{x} = (x_1, x_2, x_3)$ is extended to four dimensions by adding a zero fourth component such as $\boldsymbol{x} = (x_1, x_2, x_3, 0)$, then $\boldsymbol{x} = L(\boldsymbol{u})\boldsymbol{u}$ leads to the KS transformation $x_1 = u_1^2 - u_2^2 - u_3^2 + u_4^2$, $x_2 = 2u_1u_2 - 2u_3u_4$, $x_3 = 2u_1u_3 + 2u_2u_4$, with the fourth component equal to zero. $L'(\boldsymbol{u}) = L(\boldsymbol{u}')$ still holds as in the two-dimensional case, but $L(\boldsymbol{u})\boldsymbol{v} = L(\boldsymbol{v})\boldsymbol{u}$ requires that $u_4v_1 - u_3v_2 + u_2v_3 - u_1v_4 = 0$. This condition is called the bilinear relation that any two vectors $\boldsymbol{u}$ and $\boldsymbol{v}$ must satisfy. If the initial conditions $\boldsymbol{x}(0)$ and $\boldsymbol{x}'(0)$ of $\boldsymbol{x}(s)$ and $\boldsymbol{x}'(s)$ are given at $s = 0$, then $\boldsymbol{u}(0)$ and $\boldsymbol{u}'(0)$ can be constructed from $\boldsymbol{x} = L(\boldsymbol{u})\boldsymbol{u}$ and Eq. (3) for $\boldsymbol{u}'$, respectively, with $\boldsymbol{u}(0)$ chosen arbitrarily among the vectors corresponding to $\boldsymbol{x}(0)$. Thus,

$$\boldsymbol{u}'(0) = [1/2|\boldsymbol{u}(0)|^2]L^T[\boldsymbol{u}(0)]\boldsymbol{x}'(0)$$

is uniquely determined. The Levi-Civita[9] expression $\boldsymbol{x}' = 2L(\boldsymbol{u})\boldsymbol{u}'$ holds true in three dimensions because, from $\boldsymbol{x} = L(\boldsymbol{u})\boldsymbol{u}$, the definition of the KS transformation, $\boldsymbol{x}' = L'(\boldsymbol{u})\boldsymbol{u} + L(\boldsymbol{u})\boldsymbol{u}' = L(\boldsymbol{u}')\boldsymbol{u} + L(\boldsymbol{u})\boldsymbol{u}'$, with $L(\boldsymbol{u}')\boldsymbol{u} = L(\boldsymbol{u})\boldsymbol{u}'$. Finally, with distance r given by $r = (\boldsymbol{u}, \boldsymbol{u})$ or $r = u_1^2 + u_2^2 + u_3^2 + u_4^2$ and from $\boldsymbol{x}' = 2L\boldsymbol{u}'$,

$$\dot{\boldsymbol{x}} = \frac{\mathrm{d}\boldsymbol{x}}{\mathrm{d}t} = \frac{\mathrm{d}\boldsymbol{x}}{\mathrm{d}s}\frac{\mathrm{d}s}{\mathrm{d}t} = \frac{\boldsymbol{x}'}{u^2} = \frac{\boldsymbol{x}'}{r} = \frac{2L\boldsymbol{u}'}{r}$$

$$\dot{x}_1 = (2/r)(u_1u_1' - u_2u_2' - u_3u_3' + u_4u_4') \tag{4}$$

$$\dot{x}_2 = (2/r)(u_2u_1' + u_1u_2' - u_4u_3' - u_3u_4') \tag{5}$$

$$\dot{x}_3 = (2/r)(u_3u_1' + u_4u_2' + u_1u_3' + u_2u_4') \tag{6}$$

The initial conditions for $\boldsymbol{u}$, $\boldsymbol{u}'$, and t, at $s = 0$, needed to start the integration are obtained from the knowledge of $\boldsymbol{x}$ and $\dot{\boldsymbol{x}}$ at $t = 0$. Also, from $\dot{\boldsymbol{x}} = 2L\boldsymbol{u}'/r$,

$$u_1' = \tfrac{1}{2}(u_1\dot{x}_1 + u_2\dot{x}_2 + u_3\dot{x}_3) \tag{7}$$

$$u_2' = \tfrac{1}{2}(-u_2\dot{x}_1 + u_1\dot{x}_2 + u_4\dot{x}_3) \tag{8}$$

$$u_3' = \tfrac{1}{2}(-u_3\dot{x}_1 - u_4\dot{x}_2 + u_1\dot{x}_3) \tag{9}$$

$$u_4' = \tfrac{1}{2}(u_4\dot{x}_1 - u_3\dot{x}_2 + u_2\dot{x}_3) \tag{10}$$

Equations of Motion in Rotating Barycentric Coordinates

The three second-order differential equations of the classical restricted circular three-body problem in terms of rotating barycentric coordinates are briefly derived, and the various normalizations adopted by the researchers are introduced in this section. Let $\hat{X}$, $\hat{Y}$, and $\hat{Z}$ represent an inertial coordinate frame with $\hat{X}$ and $\hat{Y}$ contained in the plane of motion of the two primaries P_1 and P_2 (Fig. 1), and let $\hat{x}$, $\hat{y}$, and $\hat{z}$ represent a rotating frame with the $\hat{x}$ axis along the P_1P_2 direction and making an angle θ with the inertial $\hat{X}$ direction.[6] Both frames are centered at B, the barycenter of the P_1P_2 pair. The spacecraft at P_3 is located by its position vector $\boldsymbol{\rho}$ with respect to the barycenter such that $\boldsymbol{\rho} = x\hat{x} + y\hat{y} + z\hat{z}$. From the expression for the velocity $\dot{\boldsymbol{\rho}}_I = \dot{\boldsymbol{\rho}}_R + \boldsymbol{\omega} \times \boldsymbol{\rho}$, where $\boldsymbol{\omega} = \dot{\theta}\hat{z}$ is the angular rate of the rotating coordinate system, the well-known acceleration expression is obtained:

$$\ddot{\boldsymbol{\rho}} = (\ddot{x} - \ddot{\theta}y - 2\dot{\theta}\dot{y} - \dot{\theta}^2x)\hat{x} + (\ddot{y} + \ddot{\theta}x + 2\dot{\theta}\dot{x} - \dot{\theta}^2y)\hat{y} + \ddot{z}\hat{z} \tag{11}$$

which can also be written as

$$\ddot{\boldsymbol{\rho}} = -\frac{(1-\mu)}{\mathrm{d}^3}\mathbf{d} - \frac{\mu}{r^3}\boldsymbol{r} \tag{12}$$

where $\mu = m_2/(m_1 + m_2)$ and $m_1 + m_2 = 1$, and where the masses of the bodies at P_1 and P_2 are given, respectively, by $m_1 = 1 - \mu$ and $m_2 = \mu$. From the definition of the barycenter, $m_1\mathrm{d}_1 = m_2\mathrm{d}_2 = m_2(R^* - \mathrm{d}_1)$, it follows that $(m_1 + m_2)\mathrm{d}_1 = m_2R^*$, such that $\mathrm{d}_1 = [m_2R^*/(m_1 + m_2)]$, and $\mathrm{d}_2 = [m_1R^*/(m_1 + m_2)]$. Thus, $\mathbf{d} = \boldsymbol{\rho} - \mathbf{d}_1$ and $\boldsymbol{r} = \boldsymbol{\rho} - \mathbf{d}_2$ with $\mathbf{d}_1 = -\mu R^*\hat{x}$ and $\mathbf{d}_2 = (1-\mu)R^*\hat{x}$ such that $\mathbf{d} = (x + \mu R^*)\hat{x} + y\hat{y} + z\hat{z}$ and $\boldsymbol{r} = [x - (1-\mu)R^*]\hat{x} + y\hat{y} + z\hat{z}$. These expressions are used in Eq. (12), which is then equated with Eq. (11), thereby providing the equations of motion of P_3, the spacecraft, in rotating barycentric coordinates after setting $\ddot{\theta} = 0$ and thereby assuming circular motion[6] for the two massive bodies at P_1 and P_2:

$$\ddot{x} - 2\dot{\theta}\dot{y} - \dot{\theta}^2x = -\frac{(1-\mu)(x + \mu R^*)}{\mathrm{d}^3} - \frac{\mu[x - (1-\mu)R^*]}{r^3} \tag{13}$$

$$\ddot{y} + 2\dot{\theta}\dot{x} - \dot{\theta}^2y = -\frac{(1-\mu)y}{\mathrm{d}^3} - \frac{\mu y}{r^3} \tag{14}$$

$$\ddot{z} = -\frac{(1-\mu)z}{\mathrm{d}^3} - \frac{\mu z}{r^3} \tag{15}$$

In the circular restricted problem, $R^* = 1$ and $\dot{\theta} = 1$. The given quantities are nondimensional and the derivatives are with respect to nondimensional time. The angular rate of the rotating frame $n = [G(m_1 + m_2)/R^{*3}]^{1/2}$ is also nondimensional and equal to $\dot{\theta} = 1$ because G, the gravitational constant, $(m_1 + m_2)$, as well as R^* are equal to one.

Regularization of the Equations of Motion in L_1-Centered Rotating System

The circular restricted three-body equations of motion referred to the L_1 Lagrange point (to be given[1]) are regularized in this section

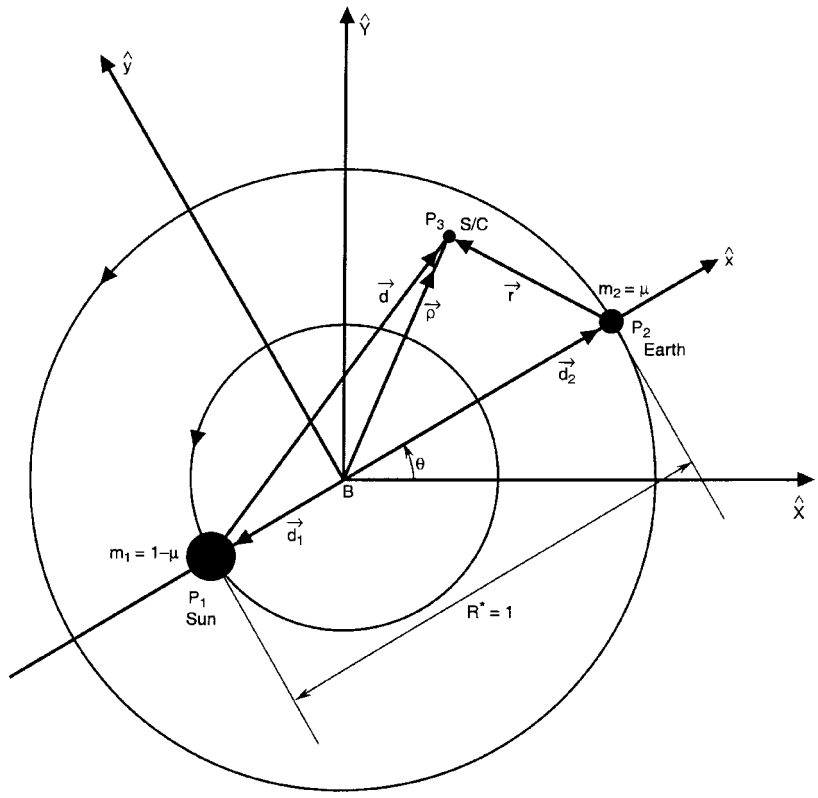

Fig. 1 Inertial and rotating frames for the sun–Earth system.[6]

following the analysis carried out in Refs. 5 and 6 that was applied to the barycentric coordinates:

$$\ddot{x} = 2\dot{y} + (1-\gamma_L) + x - \left[(1-\mu)/r_1^3\right][(1-\gamma_L)+x] + \left(\mu/r_2^3\right)(\gamma_L - x) - \mu \tag{16}$$

$$\ddot{y} = -2\dot{x} + y - \left[(1-\mu)/r_1^3\right]y - \left(\mu/r_2^3\right)y \tag{17}$$

$$\ddot{z} = -\left[(1-\mu)/r_1^3\right]z - \left(\mu/r_2^3\right)z \tag{18}$$

where μ and $(1-\mu)$ are the dimensionless masses of the Earth and the sun, respectively, and where γ_L is the distance between L_1 and the Earth and $\boldsymbol{r}_1 = \mathbf{d}$ and $\boldsymbol{r}_2 = \boldsymbol{r}$ with

$$r_1 = \left\{[(1-\gamma_L)+x]^2 + y^2 + z^2\right\}^{\frac{1}{2}}, \qquad r_2 = \left[(x-\gamma_L)^2 + y^2 + z^2\right]^{\frac{1}{2}}$$

The rotating coordinates x, y, and z are dimensionless with their first- and second-order derivatives taken with respect to the nondimensional time τ'. These equations of motion are transformed to the form where the derivatives are with respect to the physical time t in units of seconds by using

$$\frac{\mathrm{d}x}{\mathrm{d}\tau'} = \frac{1}{n_E}\frac{\mathrm{d}x}{\mathrm{d}t}, \qquad \frac{\mathrm{d}^2x}{\mathrm{d}\tau'^2} = \frac{1}{n_E^2}\frac{\mathrm{d}^2x}{\mathrm{d}t^2}, \text{ etc.}$$

such that with $n_E = 1.990986606 \times 10^{-7}$ rad/s representing the angular rate of the Earth–sun line,

$$\ddot{x} = 2n_E\dot{y} + (1-\gamma_L)n_E^2 + n_E^2 x - \left[(1-\mu)/r_1^3\right][(1-\gamma_L)+x]n_E^2 + \left(\mu/r_2^3\right)(\gamma_L - x)n_E^2 - \mu n_E^2 \tag{19}$$

$$\ddot{y} = -2n_E\dot{x} + yn_E^2 - \left[(1-\mu)/r_1^3\right]n_E^2 y - \left(\mu/r_2^3\right)n_E^2 y \tag{20}$$

$$\ddot{z} = -\left[(1-\mu)/r_1^3\right]n_E^2 z - \left(\mu/r_2^3\right)n_E^2 z \tag{21}$$

The independent variable transformation $\mathrm{d}t = r_2\mathrm{d}\tau$ is used as the first step in regularizing these differential equations such that r_2 is allowed to go to zero after the regularization is completed. From $\dot{x} = x'/r_2$ and $\ddot{x} = -(r_2'x'/r_2^3) + (1/r_2^2)x''$ and with similar expressions for the y and z variables, where the prime indicates differentiation with respect to τ, the differential equations reduce to

$$x'' = 2n_E r_2 y' + \left(x'/r_2^2\right)(\boldsymbol{r}_2\cdot\boldsymbol{r}_2') + (\mu/r_2)(\gamma_L - x)n_E^2 + r_2^2\left\{(1-\gamma_L) \times n_E^2 + n_E^2 x - \left[(1-\mu)/r_1^3\right][(1-\gamma_L)+x]n_E^2 - \mu n_E^2\right\} \tag{22}$$

$$y'' = -2n_E r_2 x' + \left(y'/r_2^2\right)(\boldsymbol{r}_2\cdot\boldsymbol{r}_2') - (\mu/r_2)n_E^2 y + r_2^2\left\{yn_E^2 - \left[(1-\mu)/r_1^3\right]n_E^2 y\right\} \tag{23}$$

$$z'' = \left(z'/r_2^2\right)(\boldsymbol{r}_2\cdot\boldsymbol{r}_2') - (\mu/r_2)n_E^2 z + r_2^2\left\{-\left[(1-\mu)/r_1^3\right]n_E^2 z\right\} \tag{24}$$

with $\boldsymbol{r}_2\cdot\boldsymbol{r}_2' = -(\gamma_L - x)x' + yy' + zz'$ because $\boldsymbol{r}_2 = [(-\gamma_L + x), y, z]^T$ and $\boldsymbol{r}_2' = (x', y', z')^T$. As in Ref. 6, let $\boldsymbol{R} = (x^*, y, z, 0)^T$, $\boldsymbol{R}' = (x', y', z', 0)^T$, and $\boldsymbol{u} = (u_1, u_2, u_3, u_4)^T$ with $x^* = x - \gamma_L$ and $x^{*'} = x'$ and $x^{*''} = x''$ and let

$$F_1^* = (1-\gamma_L)n_E^2 + n_E^2 x - \left[(1-\mu)/r_1^3\right][(1-\gamma_L)+x]n_E^2 - \mu n_E^2 \tag{25}$$

$$F_2^* = yn_E^2 - \left[(1-\mu)/r_1^3\right]n_E^2 y \tag{26}$$

$$F_3^* = -\left[(1-\mu)/r_1^3\right]n_E^2 z \tag{27}$$

The differential equations can be cast in the same form as in Ref. 6 if B is replaced by $\bar{B}$ and μ by $\bar{\mu}$

$$\boldsymbol{R}'' = (\boldsymbol{R}\cdot\boldsymbol{R}'/\boldsymbol{R}\cdot\boldsymbol{R})\boldsymbol{R}' + n_E R B\boldsymbol{R}' - n_E^2\mu(\boldsymbol{R}/R) + R^2\boldsymbol{F}^*$$

$$\bar{B} = n_E B = n_E\begin{pmatrix} 0 & 2 & 0 & 0 \\ -2 & 0 & 0 & 0 \\ 0 & 0 & 0 & 0 \\ 0 & 0 & 0 & 0 \end{pmatrix}$$

$$\bar{\mu} = n_E^2\mu, \qquad \boldsymbol{F}^* = \left(F_1^*, F_2^*, F_3^*, 0\right)^T$$

The expression for $h = (\dot{\boldsymbol{R}} \cdot \dot{\boldsymbol{R}})/2 - \mu/R$ in Ref. 6, which is needed in the second-order differential equation for $\boldsymbol{u}$ to be given is replaced by

$$\bar{h} = \frac{2L(\boldsymbol{u})\boldsymbol{u}' \cdot L(\boldsymbol{u})\boldsymbol{u}'}{R^2} - \frac{\bar{\mu}}{R} = \frac{2(\boldsymbol{u}' \cdot \boldsymbol{u}') - \bar{\mu}}{\boldsymbol{u} \cdot \boldsymbol{u}}$$

such that the vector differential equation[6] has the form

$$\boldsymbol{u}'' = (\bar{h}/2)\boldsymbol{u} + L^T(\boldsymbol{u})\bar{B}L(\boldsymbol{u})\boldsymbol{u}' + [(\boldsymbol{u} \cdot \boldsymbol{u})]/2]L^T(\boldsymbol{u})\boldsymbol{F}^* \tag{28}$$

This form is obtained from the preceding $\boldsymbol{R}''$ equation because $R = \boldsymbol{u} \cdot \boldsymbol{u}$, $L^T(\boldsymbol{u})L(\boldsymbol{u}) = RI$, and $\boldsymbol{R}' = 2L(\boldsymbol{u})\boldsymbol{u}'$. The Jacobi constant is unitless and is given by $C_J = 2U^* - (\dot{x}^2 + \dot{y}^2 + \dot{z}^2)$. However, if the physical time is adopted as the independent variable, then $\dot{x}$, etc., will have the dimension per second, and it is then necessary to write C_J as $C_J = 2U^* - [\dot{x}^2/n_E^2 + \dot{y}^2/n_E^2 + \dot{z}^2/n_E^2]$ with U^*, the pseudopotential, given by

$$U^* = \tfrac{1}{2}\left(x_B^2 + y_B^2\right) + (1-\mu)/\mathrm{d} + \mu/r$$

The barycentric coordinates x_B and y_B are unitless, and they are related to the unitless x and y coordinates by $x_B = x + [(1-\mu) - \gamma_L]$ and $y_B = y$. Thus,

$$U^* = \tfrac{1}{2}\left\{[x + (1-\mu) - \gamma_L]^2 + y^2\right\} + (1-\mu)/\mathrm{d} + \mu/r$$

with $\mathrm{d} = r_1$ and $r = r_2$ also unitless. From

$$\bar{h} = \tfrac{1}{2}(\dot{x}^2 + \dot{y}^2 + \dot{z}^2) - n_E^2\mu/r = \tfrac{1}{2}\dot{\boldsymbol{R}} \cdot \dot{\boldsymbol{R}} - \bar{\mu}/R$$

and with physical time as the independent variable, it follows that

$$\bar{h} = n_E^2(U^* - C_J/2) - n_E^2\mu/r$$

which reduces to

$$\bar{h} = n_E^2\left(\tfrac{1}{2}\left\{[x + (1-\mu) - \gamma_L]^2 + y^2\right\} + (1-\mu)/\mathrm{d} - C_J/2\right) \tag{29}$$

where $\bar{h}$ has units of per second squared and is suitable for use in the differential equations for the u_j parameters in Eq. (28), now nonsingular. Finally, from $\boldsymbol{R} = L(\boldsymbol{u})\boldsymbol{u}$, it follows that $x^* = u_1^2 - (u_2^2 + u_3^2 - u_4^2)$, $y = 2u_1u_2 - 2u_3u_4$, $z = 2u_1u_3 + 2u_2u_4$, and $(x^{*^2} + y^2 + z^2)^{1/2} = u_1^2 + u_2^2 + u_3^2 + u_4^2 = \boldsymbol{u} \cdot \boldsymbol{u} = R$. The second-order differential equations in the u variables

$$\begin{pmatrix} u_1'' \\ u_2'' \\ u_3'' \\ u_4'' \end{pmatrix} = \frac{\bar{h}}{2}\begin{pmatrix} u_1 \\ u_2 \\ u_3 \\ u_4 \end{pmatrix} + 2n_E \times \begin{bmatrix} \left(u_1^2 + u_2^2\right)u_2' + (u_2u_3 - u_1u_4)u_3' - (u_1u_3 + u_2u_4)u_4' \\ -\left(u_1^2 + u_2^2\right)u_1' + (u_2u_4 + u_1u_3)u_3' + (u_2u_3 - u_1u_4)u_4' \\ (u_1u_4 - u_2u_3)u_1' - (u_1u_3 + u_2u_4)u_2' + \left(u_3^2 + u_4^2\right)u_4' \\ (u_2u_4 + u_1u_3)u_1' + (u_1u_4 - u_2u_3)u_2' - \left(u_3^2 + u_4^2\right)u_3' \end{bmatrix}$$

$$+ \frac{1}{2}\left(u_1^2 + u_2^2 + u_3^2 + u_4^2\right)\begin{pmatrix} u_1F_1^* + u_2F_2^* + u_3F_3^* \\ -u_2F_1^* + u_1F_2^* + u_4F_3^* \\ -u_3F_1^* - u_4F_2^* + u_1F_3^* \\ u_4F_1^* - u_3F_2^* + u_2F_3^* \end{pmatrix}$$

are equivalent to the following eight first-order differential equations:

$$u_1' = v_1 \tag{30}$$

$$u_2' = v_2 \tag{31}$$

$$u_3' = v_3 \tag{32}$$

$$u_4' = v_4 \tag{33}$$

$$v_1' = (\bar{h}/2)u_1 + 2n_E\left[\left(u_1^2 + u_2^2\right)v_2 + \left(u_2u_3 - u_1u_4\right)v_3 - \left(u_1u_3 + u_2u_4\right)v_4\right] + \tfrac{1}{2}\left(u_1^2 + u_2^2 + u_3^2 + u_4^2\right)\left(u_1F_1^* + u_2F_2^* + u_3F_3^*\right) \tag{34}$$

$$v_2' = (\bar{h}/2)u_2 + 2n_E\left[-\left(u_1^2 + u_2^2\right)v_1 + (u_2u_4 + u_1u_3)v_3 + (u_2u_3 - u_1u_4)v_4\right] + \tfrac{1}{2}\left(u_1^2 + u_2^2 + u_3^2 + u_4^2\right)\left(-u_2F_1^* + u_1F_2^* + u_4F_3^*\right) \tag{35}$$

$$v_3' = (\bar{h}/2)u_3 + 2n_E\left[(u_1u_4 - u_2u_3)v_1 - (u_1u_3 + u_2u_4)v_2 + \left(u_3^2 + u_4^2\right)v_4\right] + \tfrac{1}{2}\left(u_1^2 + u_2^2 + u_3^2 + u_4^2\right)\left(-u_3F_1^* - u_4F_2^* + u_1F_3^*\right) \tag{36}$$

$$v_4' = (\bar{h}/2)u_4 + 2n_E\left[(u_2u_4 + u_1u_3)v_1 + (u_1u_4 - u_2u_3)v_2 - \left(u_3^2 + u_4^2\right)v_3\right] + \tfrac{1}{2}\left(u_1^2 + u_2^2 + u_3^2 + u_4^2\right)\left(u_4F_1^* - u_3F_2^* + u_2F_3^*\right) \tag{37}$$

Because the integration is with respect to the fictitious time τ, it is also necessary to integrate, simultaneously with the preceding eight differential equations, the equation for the physical time t, that is,

$$\frac{\mathrm{d}t}{\mathrm{d}\tau} = u_1^2 + u_2^2 + u_3^2 + u_4^2 \tag{38}$$

From the expressions for x^*, y, and z in terms of u_1, u_2, u_3, and u_4, it can be shown[10] that, if $x^* > 0$, then

$$u_1^2 + u_4^2 = \frac{1}{2}(r + x^*) \tag{39}$$

$$u_2 = \frac{yu_1 + zu_4}{r + x^*} \tag{40}$$

$$u_3 = \frac{zu_1 - yu_4}{r + x^*} \tag{41}$$

and if $x^* < 0$, then

$$u_2^2 + u_3^2 = \frac{1}{2}(r - x^*) \tag{42}$$

$$u_1 = \frac{yu_2 + zu_3}{r - x^*} \tag{43}$$

$$u_4 = \frac{zu_2 - yu_3}{r - x^*} \tag{44}$$

If $x^* > 0$, u_1 can be selected arbitrarily and u_4 solved for from Eq. (39). Then u_2 and u_3 are obtained from Eqs. (40) and (41), respectively. For $x^* < 0$, u_2 is selected arbitrarily, then u_3 is determined from Eq. (42), after which u_1 and u_4 are evaluated from Eqs. (43) and (44). These manipulations are needed to initialize the integration at $\tau = 0$ because, at time $t = 0$, we are given x, y, z, $\dot{x}$, $\dot{y}$, and $\dot{z}$, or $x(0)$, $y(0)$, $z(0)$, $\dot{x}(0)$, $\dot{y}(0)$, and $\dot{z}(0)$. Once $u_1(0)$, $u_2(0)$, $u_3(0)$, and $u_4(0)$ are determined from Eqs. (39–44), the velocities $u_1'(0)$, $u_2'(0)$, $u_3'(0)$, and $u_4'(0)$ needed to start the integration are obtained from Eqs. (7–10) evaluated at $\tau = 0$. These equations are obtained from the velocity equations for $\dot{x}^*$, $\dot{y}$, and $\dot{z}$ with, for example, $\dot{x}^* = (2/r_2)(u_1u_1' - u_2u_2' - u_3u_3' + u_4u_4')$. This expression for $\dot{x}^*$ is readily obtained from $x^* = u_1^2 - u_2^2 - u_3^2 + u_4^2$, or

$$\dot{x}^* = 2u_1u_1'\frac{\mathrm{d}\tau}{\mathrm{d}t} - 2u_2u_2'\frac{\mathrm{d}\tau}{\mathrm{d}t} - 2u_3u_3'\frac{\mathrm{d}\tau}{\mathrm{d}t} + 2u_4u_4'\frac{\mathrm{d}\tau}{\mathrm{d}t}$$

where $\mathrm{d}\tau/\mathrm{d}t = 1/r_2$. The expressions for $\dot{y}$ and $\dot{z}$ are obtained likewise by differentiation of y and z. The equations of motion in terms of the parameters u_j that are related to the rotating Cartesian coordinates centered at L_1 are, thus, regularized allowing the trajectory to approach the Earth without experiencing any singularity-associated numerical roundoff and truncation errors during the integration.

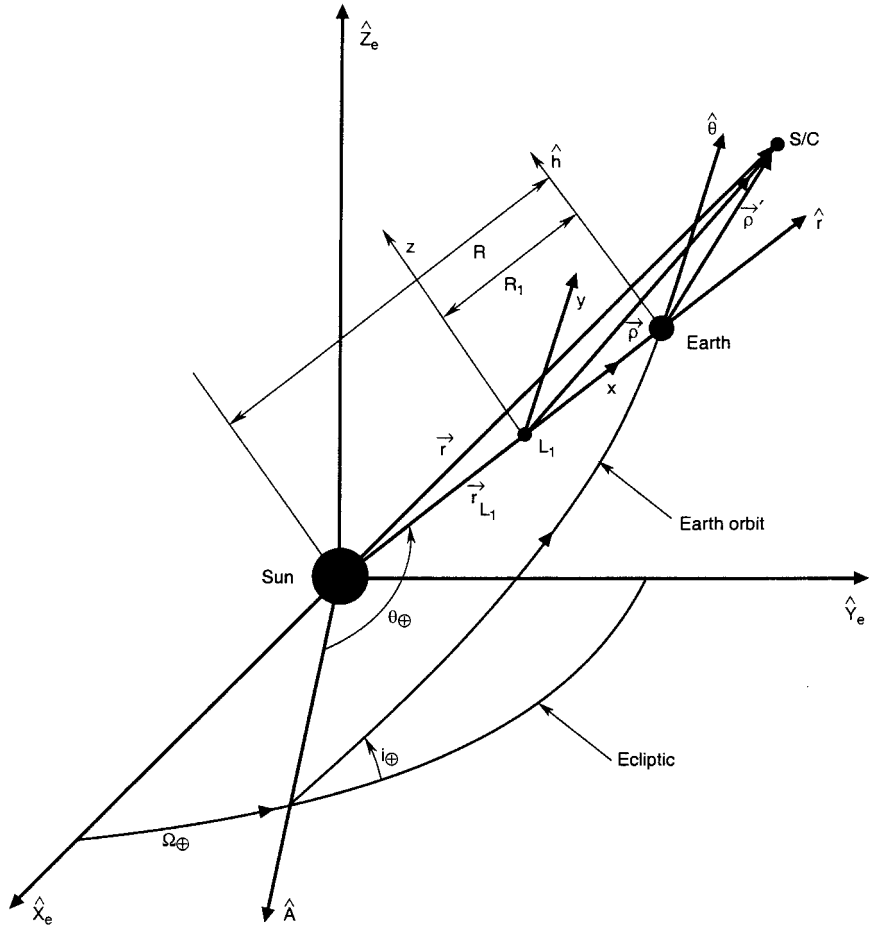

Fig. 2 Earth geometry in sun-centered system.

Numerical Simulations

The importance of the regularization is shown in this section by directly comparing integrated paths that use either the singular system or the regularized one. The details of the initialization of the integrations are also shown, and the integration criteria for the generation of an accurate transfer solution are further discussed. A family of solutions that meet the end or boundary conditions is generated for a transfer from LEO to a given point on a typical size halo orbit with high accuracy.

Forward Integration

Let $\hat{X}_{\text{eq}}$, $\hat{Y}_{\text{eq}}$, and $\hat{Z}_{\text{eq}}$ be an Earth-centered inertial equatorial system, and let i_s be the sun's apparent orbit equatorial inclination, also called the obliquity of the ecliptic. The sun's apparent orbit position is given by $\theta_\odot$ with $\delta_\odot$ and $\lambda_\odot$ representing the solar declination and longitude, respectively. Let us now assume a tangential injection from a circular LEO whose altitude is h_p and radial distance from the center of the Earth $r_p = h_p + 6378.14$ km. The circular orbital velocity is given by $V_c = (\mu_e/r_p)^{1/2}$, where $\mu_e = 398{,}601.3\ \text{km}^3/\text{s}^2$ is the Earth gravity constant. Given a ΔV_{inj} at injection, the post-ΔV_{inj} velocity at perigee is $Vp = V_c + \Delta V_{\text{inj}}$, and from the energy equation the postinjection orbit semimajor axis is obtained as

$$a_0 = \frac{\mu_e}{2\left(\mu_e/r_p - V_p^2/2\right)}$$

and its eccentricity from $e_0 = 1 - r_p/a_0$. The initial values of a_0, e_0, ω_0, and Ω_0 needed for a transfer orbit to reach the vicinity of the Lagrange L_1 point are guessed to reach a target point on a given halo orbit. A forward integration can be carried out by using the nonregularized equations of motion, namely, Eqs. (16–18). These differential equations are transformed to a form where the derivatives are with respect to the physical time t, by using $\mathrm{d}x/\mathrm{d}\tau' = (1/n_E)(\mathrm{d}x/\mathrm{d}t)$ and $\mathrm{d}^2x/\mathrm{d}\tau'^2 = (1/n_E^2)(\mathrm{d}^2x/\mathrm{d}t^2)$, and so on.

As in Ref. 1, let $\mu = GM_1 = M_1/(M_1 + M_2)$ with M_2 the mass of the sun and M_1 the combined masses of the Earth and the moon, $M_1 = M_\oplus + M_\leftmoon$ such that $\mu = 3.040357143 \times 10^{-6}$. Also, $R_1 = 1.497610042 \times 10^6$ km is the L_1–Earth distance shown in Fig. 2, and $a_1 = 1.495978714 \times 10^8$ km (one astronomical unit or the mean sun–Earth distance). The value of $\gamma_L = 1.001090475 \times 10^{-2}$ is a dimensionless quantity and is equal to R_1/a_1. The initial values of x, y, z, $\dot{x}$, $\dot{y}$, and $\dot{z}$ to start the numerical integrations from the given injection point are obtained subsequently. Figure 2 shows the sun-centered ecliptic system with the Earth angular position $\theta_\oplus$ measured from its ascending node with $\Omega_\oplus$ and $i_\oplus$ the other Eulerian angles. The spacecraft is located by the vector $\boldsymbol{\rho}$ from the L_1 point and $\boldsymbol{\rho}'$ from the Earth center. The rotating $\hat{r}$, $\hat{\theta}$, $\hat{h}$ and x, y, z frames are parallel and attached, respectively, to the Earth and L_1. The rotation from $\hat{r}$, $\hat{\theta}$, $\hat{h}$ to the ecliptic is performed by

$$\begin{pmatrix} \hat{X}_e \\ \hat{Y}_e \\ \hat{Z}_e \end{pmatrix} =$$

$$\begin{pmatrix} c_{\Omega_\oplus}c_{\theta_\oplus} - s_{\Omega_\oplus}c_{i_\oplus}s_{\theta_\oplus} & -c_{\Omega_\oplus}s_{\theta_\oplus} - s_{\Omega_\oplus}c_{i_\oplus}c_{\theta_\oplus} & s_{\Omega_\oplus}s_{i_\oplus} \\ s_{\Omega_\oplus}c_{\theta_\oplus} + c_{\Omega_\oplus}c_{i_\oplus}s_{\theta_\oplus} & -s_{\Omega_\oplus}s_{\theta_\oplus} + c_{\Omega_\oplus}c_{i_\oplus}c_{\theta_\oplus} & -c_{\Omega_\oplus}s_{i_\oplus} \\ s_{i_\oplus}s_{\theta_\oplus} & s_{i_\oplus}c_{\theta_\oplus} & c_{i_\oplus} \end{pmatrix} \begin{pmatrix} \hat{r} \\ \hat{\theta} \\ \hat{h} \end{pmatrix}$$

or

$$\begin{pmatrix} \hat{X}_e \\ \hat{Y}_e \\ \hat{Z}_e \end{pmatrix} = \begin{pmatrix} A_\oplus & C_\oplus & G_\oplus \\ B_\oplus & D_\oplus & H_\oplus \\ E_\oplus & F_\oplus & K_\oplus \end{pmatrix} \begin{pmatrix} \hat{r} \\ \hat{\theta} \\ \hat{h} \end{pmatrix} = R_{\Omega_\oplus i_\oplus \theta_\oplus} \begin{pmatrix} \hat{r} \\ \hat{\theta} \\ \hat{h} \end{pmatrix}$$

The symbols s and c are used throughout the paper to denote sin and cos. From $\boldsymbol{r} = \boldsymbol{R} + \boldsymbol{\rho}'$ and $\boldsymbol{v} = \dot{\boldsymbol{R}} + \dot{\boldsymbol{\rho}}'$ with $\dot{\boldsymbol{\rho}}' = \dot{\boldsymbol{\rho}}_I + (\boldsymbol{\omega}_I \times \boldsymbol{\rho}'_I)$, where $\dot{\boldsymbol{\rho}}'_I = (\dot{x}'_I \;\; \dot{y}'_I \;\; \dot{z}'_I)^T$ and $\boldsymbol{\rho}'_I = (\rho'_{\hat{X}_e} \;\; \rho'_{\hat{Y}_e} \;\; \rho'_{\hat{Z}_e})^T$, and where the angular velocity of the Earth is given by $\boldsymbol{\omega}_I = R_{\Omega_\oplus i_\oplus \theta_\oplus} \boldsymbol{\omega}_R$ with $\boldsymbol{\omega}_R =$

$[0\ 0\ (h_\oplus/R^2)]^T$, $\rho'_{\hat{X}_e} = A_\oplus x' + C_\oplus y' + G_\oplus z'$, $\rho'_{\hat{Y}_e} = B_\oplus x' + D_\oplus y' + H_\oplus z'$, and $\rho'_{\hat{Z}_e} = E_\oplus x' + F_\oplus y' + K_\oplus z'$. Also, $\boldsymbol{R} = R(A_\oplus B_\oplus E_\oplus)^T$ and $\dot{\boldsymbol{R}} = \mu_\odot/h_\oplus (C_\oplus D_\oplus F_\oplus)^T$, and

$$\begin{pmatrix} \dot{x}'_I \\ \dot{y}'_I \\ \dot{z}'_I \end{pmatrix} = \begin{pmatrix} A_\oplus & C_\oplus & G_\oplus \\ B_\oplus & D_\oplus & H_\oplus \\ E_\oplus & F_\oplus & K_\oplus \end{pmatrix} \begin{pmatrix} \dot{x}' \\ \dot{y}' \\ \dot{z}' \end{pmatrix}, \qquad \begin{pmatrix} \dot{x}' \\ \dot{y}' \\ \dot{z}' \end{pmatrix} = \begin{pmatrix} \dot{x} \\ \dot{y} \\ \dot{z} \end{pmatrix}$$

The ecliptic position and velocity components of the spacecraft are given by

$$X_e = RA_\oplus + \rho'_{\hat{X}_e}, \qquad Y_e = RB_\oplus + \rho'_{\hat{Y}_e}, \qquad Z_e = RE_\oplus + \rho'_{\hat{Z}_e}$$

$$\dot{X}_e = \mu_\odot/h_\oplus C_\oplus + (A_\oplus \dot{x}' + C_\oplus \dot{y}' + G_\oplus \dot{z}') - \left(h_\oplus/R^2\right)\left(c_{\Omega_\oplus} s_{i_\oplus} \rho'_{\hat{Z}_e} + c_{i_\oplus} \rho'_{\hat{Y}_e}\right)$$

$$\dot{Y}_e = \mu_\odot/h_\oplus D_\oplus + (B_\oplus \dot{x}' + D_\oplus \dot{y}' + H_\oplus \dot{z}') - \left(h_\oplus/R^2\right)\left(s_{\Omega_\oplus} s_{i_\oplus} \rho'_{\hat{Z}_e} + c_{i_\oplus} \rho'_{\hat{X}_e}\right)$$

$$\dot{Z}_e = \mu_\odot/h_\oplus F_\oplus + (E_\oplus \dot{x}' + F_\oplus \dot{y}' + K_\oplus \dot{z}') + \left(h_\oplus/R^2\right)\left(s_{\Omega_\oplus} s_{i_\oplus} \rho'_{\hat{Y}_e} + c_{\Omega_\oplus} s_{i_\oplus} \rho'_{\hat{X}_e}\right)$$

In the preceding equations, $\mu_\odot$ is the gravity constant of the sun, $h_\oplus$ is the orbital angular momentum of the Earth, and $h_\oplus/R^2 = \dot{\theta}_\oplus = n_E$. The coordinates x and x' are related by the relation $x = x' + R_1$ whereas $y = y'$ and $z = z'$. The quantities $\dot{x}'_I$, $\dot{y}'_I$, and $\dot{z}'_I$ are the relative velocity components as observed in the rotating $\hat{r}, \hat{\theta}, \hat{h}$ frame but measured along the inertial ecliptic axes $\hat{X}_e$, $\hat{Y}_e$, and $\hat{Z}_e$. If the $\boldsymbol{R}$ and $\dot{\boldsymbol{R}}$ parts in the $\boldsymbol{r}$ and $\boldsymbol{v}$ equations are removed, then the position and velocity components of the spacecraft in the inertial Earth-centered ecliptic system $\hat{X}'_e$, $\hat{Y}'_e$, and $\hat{Z}'_e$ whose axes are parallel to the inertial $\hat{X}_e$, $\hat{Y}_e$, and $\hat{Z}_e$ axes will be given by X'_e, Y'_e, Z'_e, $\dot{X}'_e$, $\dot{Y}'_e$, and $\dot{Z}'_e$. A rotation through the angle $\varepsilon = i_s$, also called the obliquity of the ecliptic and given by the rotation matrix,

$$T = \begin{pmatrix} 1 & 0 & 0 \\ 0 & c_\varepsilon & s_\varepsilon \\ 0 & -s_\varepsilon & c_\varepsilon \end{pmatrix}$$

will rotate the position vector into the equatorial Earth-centered system $\hat{X}_{\text{eq}}$, $\hat{Y}_{\text{eq}}$, and $\hat{Z}_{\text{eq}}$. From $(\hat{X}'_e\ \hat{Y}'_e\ \hat{Z}'_e)^T = T(\hat{X}_{\text{eq}}\ \hat{Y}_{\text{eq}}\ \hat{Z}_{\text{eq}})^T$,

$$\begin{pmatrix} X_{\text{eq}} \\ Y_{\text{eq}} \\ Z_{\text{eq}} \end{pmatrix} = T^{-1} \begin{pmatrix} X'_e \\ Y'_e \\ Z'_e \end{pmatrix} \tag{45}$$

whereas the velocity vector is rotated through $(\dot{X}'_e\ \dot{Y}'_e\ \dot{Z}'_e)^T = T(\dot{X}_{\text{eq}}\ \dot{Y}_{\text{eq}}\ \dot{Z}_{\text{eq}})^T + \dot{T}(X_{\text{eq}}\ Y_{\text{eq}}\ Z_{\text{eq}})^T$. If we assume that $\dot{\varepsilon} = 0$ or that i_s remains constant, then $\dot{T} = 0$ and

$$\begin{pmatrix} \dot{X}_{\text{eq}} \\ \dot{Y}_{\text{eq}} \\ \dot{Z}_{\text{eq}} \end{pmatrix} = T^{-1} \begin{pmatrix} \dot{X}'_e \\ \dot{Y}'_e \\ \dot{Z}'_e \end{pmatrix} \tag{46}$$

If we assume $i_\oplus = \Omega_\oplus = 0$ such that the Earth orbit is located exactly within the ecliptic, then

$$\begin{pmatrix} x' \\ y' \\ z' \end{pmatrix} = \begin{pmatrix} c_{\theta_\oplus} & s_{\theta_\oplus} & 0 \\ -s_{\theta_\oplus} & c_{\theta_\oplus} & 0 \\ 0 & 0 & 1 \end{pmatrix} \begin{pmatrix} X'_e \\ Y'_e \\ Z'_e \end{pmatrix} \tag{47}$$

$$\begin{pmatrix} \dot{x}' \\ \dot{y}' \\ \dot{z}' \end{pmatrix} = \begin{pmatrix} c_{\theta_\oplus} & s_{\theta_\oplus} & 0 \\ -s_{\theta_\oplus} & c_{\theta_\oplus} & 0 \\ 0 & 0 & 1 \end{pmatrix} \left[\begin{pmatrix} \dot{X}'_e + n_E\left(s_{\theta_\oplus} x' + c_{\theta_\oplus} y'\right) \\ \dot{Y}'_e - n_E\left(c_{\theta_\oplus} x' - s_{\theta_\oplus} y'\right) \\ \dot{Z}'_e \end{pmatrix} \right] \tag{48}$$

In summary, given the orbit elements of the post-ΔV_{inj} elliptic orbit at the injection time, namely, a_0, e_0, i_0, Ω_0, ω_0, and θ_0^* with angular position given by $\theta_r = \omega_0 + \theta_0^* = \omega_0$, the inertial equatorial coordinates corresponding to this injection point are computed first, followed by the ecliptic coordinates X'_e, Y'_e, Z'_e and $\dot{X}'_e$, $\dot{Y}'_e$, $\dot{Z}'_e$ obtained from Eqs. (45) and (46), after which x', y', z', $\dot{x}'$, $\dot{y}'$, and $\dot{z}'$ are obtained from Eqs. (47) and (48). Thus, $x = x' + R_1$, $y = y'$, $z = z'$, $\dot{x} = \dot{x}'$, $\dot{y} = \dot{y}'$, and $\dot{z} = \dot{z}'$. Also, $h_\oplus = (\mu_\odot R)^{1/2}$, $h_\oplus/R^2 = \mu_\odot^{1/2} R^{-3/2} = n_\oplus = n_E$ requires $\mu_\odot = 1.32712833 \times 10^{11}$ km^3/s^2 for the sun's gravity constant. Because the equations of motion are not regularized, a numerical experiment has been carried out to find out the sensitivity of the propagated trajectory to the integration error controls. When $a_0 = 565{,}000$ km, $i_0 = 28.5$ deg, $\Omega_0 = 300$ deg, $\omega_0 = 290$ deg, $\theta_0^* = 0$ deg with $\theta_\odot = 60$ deg, and $i_s = 23.440$ deg, and $h_p = 185$ km, $\theta_\oplus = \theta_\odot + 180$ deg, $\theta_r = \omega_0 + \theta_0^*$ and $t_f = 9.072 \times 10^6$ s or 105 days is used, the injection ΔV_{inj} is calculated from $e_0 = 0.988383823$ and $V_p = 10.9891381$ km/s as $\Delta V_{\text{inj}} = 3.19597940$ km/s. The initial state is calculated next, the integrator error controls set at 10^{-12}, and the trajectory integrated until t_f. The value of C_J varies appreciably near the Earth from 2.863903594 at $t = 0$ to $C_J = 2.997936272$ at $t = 1$ day. Let $\theta_\odot$ be now associated to an epoch called t_M such that $\theta_\oplus = \theta_\odot + \pi$ corresponds to the position of the Earth at time t_M. Thus, $(\theta_\oplus)_0 = (\theta_\oplus)_{t_M} - n_E(t_M - t_0)$ will provide the position of the Earth at time $t_0 = 0$. As before, given the orbit elements at time t_0, then x_0, y_0, z_0, $\dot{x}_0$, $\dot{y}_0$, and $\dot{z}_0$ are evaluated to start the integrations. Furthermore, $x_0^* = x_0 - \gamma_L$ is evaluated as well as $r_0 = (x_0^{*2} + y_0^2 + z_0^2)^{1/2}$. If $x_0^* < 0$, then $(u_3)_0$ is chosen arbitrarily as $(u_3)_0 = (-x_0^*/2)^{1/2}$, and $(u_2)_0$, $(u_1)_0$, and $(u_4)_0$ are computed from Eqs. (42–44). If $x_0^* > 0$, then $(u_4)_0 = (x_0^*/2)^{1/2}$ is chosen arbitrarily, and $(u_1)_0$, $(u_2)_0$, and $(u_3)_0$ are computed from Eqs. (39–41). The velocities $(u'_1)_0$, $(u'_2)_0$, $(u'_3)_0$, and $(u'_4)_0$ are computed next from Eqs. (7–10). The regularized differential equations in Eqs. (30–38) are integrated forward simultaneously with respect to the nondimensional time τ starting from $\tau = 0$. The bilinear relation is also calculated during the integration from $b_\ell = u_4 u'_1 - u_3 u'_2 + u_2 u'_3 - u_1 u'_4$. The trajectory is terminated at a value of τ^* that would roughly correspond to $t_f = 9.072 \times 10^6$ s. It is found that $C_J = 3.002493195$ stays constant throughout the integration and that $b_\ell = -9.0 \times 10^{-16}$ stays at 10^{-16} or less, which is effectively equal to the theoretical value of zero. However, because of the sensitivity of the terminal state near the L_1 point to small changes in the initial conditions at injection, a backward integration scheme is necessary to carry out the iterations in a successful way.

Backward Integration

The following state vector that corresponds to the initial point on a typical halo orbit is used for backward integration:

$$\begin{aligned} (x_T)_f &= 0.247378606 \times 10^6 \text{ km}, & (\dot{x}_T)_f &= 0.0 \text{ km/s} \\ (y_T)_f &= 0.0 \text{ km}, & (\dot{y}_T)_f &= -0.293231000 \text{ km/s} \\ (z_T)_f &= -0.113959359 \times 10^6 \text{ km}, & (\dot{z}_T)_f &= 0.0 \text{ km/s} \end{aligned} \tag{49}$$

This point in the vicinity of the sun–Earth L_1 point corresponds to the first x–z crossing and, when propagated forward in time, will trace the halo orbit periodically with a period of $P = 1.536671218 \times 10^7$ s or 177.8554650 days. Here $\gamma_L = 1.0011 \times 10^{-2}$ is used with otherwise the same physical constants. Now given $\theta_\oplus$, $i_\oplus$, and $\Omega_\oplus$, the values of $A_\oplus, \ldots, K_\oplus$ are first computed, after which $x' = x - \gamma_L$, $y' = y$, and $z' = z$ are evaluated, with $x = (x_T)_f$, $y = (y_T)_f$, $z = (z_T)_f$ .... Then, the coordinates $\rho'_{\hat{X}_e}$, $\rho'_{\hat{Y}_e}$, and $\rho'_{\hat{Z}_e}$ and $\dot{x}'_I$, $\dot{y}'_I$, and $\dot{z}'_I$ as well as X'_e, Y'_e, Z'_e, $\dot{X}'_e$, $\dot{Y}'_e$, and $\dot{Z}'_e$ and X_{eq}, Y_{eq}, Z_{eq}, $\dot{X}_{\text{eq}}$, $\dot{Y}_{\text{eq}}$, and $\dot{Z}_{\text{eq}}$ are computed, the latter from Eqs. (45) and (46). The backward integration is carried out by first making the change of variable from τ to τ' such that $\tau' = -\tau$ and $\mathrm{d}/\mathrm{d}\tau' = -\mathrm{d}/\mathrm{d}\tau$, $\mathrm{d}^2/\mathrm{d}\tau'^2 = \mathrm{d}^2/\mathrm{d}\tau^2$. The sign of the second term in each of Eqs. (34–37) is changed, and these equations as well as the expressions for F_1^*, F_2^*, F_3^*, and $\bar{h}$ are used without the n_E and n_E^2 factors to render all of the quantities at hand unitless.

The value of $\theta_\oplus$ at time t_f is stored as $(\theta_\oplus)_f$ and the differential equation $\mathrm{d}t/\mathrm{d}\tau$ in Eq. (38) is now replaced by

$$\frac{\mathrm{d}t}{\mathrm{d}\tau'} = -\left(u_1^2 + u_2^2 + u_3^2 + u_4^2\right) \tag{50}$$

Given t_f in seconds, time t is initialized at $t = t_f/n_E$. From $x^* = x - \gamma_L$, if $x^* > 0$, $(u_4)_0$ is chosen arbitrarily as $(u_4)_0 = (\frac{1}{2}x^*)^{1/2}$. Then $(u_1)_0$, $(u_2)_0$, and $(u_3)_0$ are evaluated as before. If $x^* < 0$, $(u_3)_0$ is chosen arbitrarily as $(u_3)_0 = (-\frac{1}{2}x^*)^{1/2}$, and $(u_2)_0$, $(u_1)_0$, and $(u_4)_0$ are also evaluated. The conversion from the u_i to x, y, z, $\dot{x}$, $\dot{y}$, and $\dot{z}$ is carried out at each interval during the integration by using Eqs. (4–6) for $\dot{x}$, $\dot{y}$, and $\dot{z}$ with a minus sign after the equal sign because u'_1, u'_2, u'_3, and u'_4, which appear linearly, are with respect to $\tau' = -\tau$ and not τ. Now, as τ' takes on increasingly larger positive values starting from $\tau' = 0$, the physical time t decreases in value starting from t_f. It is necessary to provide $\theta_\odot$ at time t_M, which will act as a master time, and compute $\theta_\oplus = \theta_\odot + \pi$. The Earth is now allowed to move in time from t_M to t_{f_0}, which is the guessed transfer time, so that the angle $\theta_\oplus$ at t_{f_0} can be evaluated from $(\theta_\oplus)_{t_{f_0}} = (\theta_\oplus)_{t_M} - n_E(t_M - t_{f_0})$. The angle $(\theta_\oplus)_{t_{f_0}}$ is now used to calculate the initial conditions at the halo point after computing the ecliptic and equatorial coordinates and, thus, the orbital elements as before. The velocities at the halo point are, of course, calculated by adding $\Delta\dot{x}$, $\Delta\dot{y}$, and $\Delta\dot{z}$, that is, the maneuver velocities to the values shown in Eq. (49), which correspond to the pre-ΔV values, or when arriving from the Earth to the post-ΔV values that capture the trajectory onto the periodic orbit. The value of t_f is initialized as $t_{f_y} = t_{f_0}/(86{,}400 \times 365.25)$ in units of years. As the value of t_{f_y} is adjusted, the Earth position $\theta_\oplus$ is also adjusted from its initial $(\theta_\oplus)_{t_{f_0}}$ value by $(\theta_\oplus)_{t_{f_y}} = (\theta_\oplus)_{t_{f_0}} - n_E(t_{f_0} - t_{f_y} \times 365.25 \times 86{,}400)$. Time t initialized as $X(9) = t_{f_y} \times 365.25 \times 86{,}400 \times n_E$ is integrated backward during each iteration, and the Earth position is also constantly adjusted with $(\theta_\oplus)_t = (\theta_\oplus)_{t_{f_y}} - (t_{f_y} \times 365.25 \times 86{,}400 \times n_E - t)$. This angle is the angle used to calculate the $A_\oplus, \ldots, K_\oplus$ elements that lead to the evaluation of the spacecraft ecliptic and equatorial coordinates, and thereby the current orbital elements corresponding to the current time t.

A double precision integrator using the Adams method for integration that has a built-in interpolator[9] is used in all subsequent runs with a requested relative accuracy in all solution components of 10^{-12} and with a 32-bit compilation for reliable and accurate results. The integration is stopped by a root-finding routine as soon as a user-provided function changes sign. A minimization software[9] is also used, and each trajectory is terminated at $\dot{r} = 0$ or $\boldsymbol{r} \cdot \boldsymbol{v} = 0$ or exactly at the perigee of the departure orbit. Of course, $\boldsymbol{r} \cdot \boldsymbol{v} = X_{\text{eq}}\dot{X}_{\text{eq}} + Y_{\text{eq}}\dot{Y}_{\text{eq}} + Z_{\text{eq}}\dot{Z}_{\text{eq}}$ is known from the knowledge of the inertial equatorial position and velocity components at each time. The termination time in general will take on values of the order of days when a trajectory is integrated with a rough initial guess for the maneuver components $\Delta\dot{x}$, $\Delta\dot{y}$, and $\Delta\dot{z}$. Furthermore, the user-provided function needed by the integrator has a builtin flag that allows for the $\boldsymbol{r} \cdot \boldsymbol{v} = 0$ interpolation to take place near the end of the trajectory or in practice some 10–30 days before the end time, to prevent the trajectory from terminating on the earlier zeros of the $\boldsymbol{r} \cdot \boldsymbol{v}$ function. A two-parameter search version is created first, which searches only on $\Delta\dot{x}$ and $\Delta\dot{y}$ leaving $\Delta\dot{z} = 0$, in order to match a desired h_T and ω_T at the LEO injection point. Because the angular position of the Earth $\theta_\oplus$ corresponds to t_{f_0}, and because the trajectory does not end exactly at $t = 0$, the value of t_{f_0} that results in $t = 0$ at the end of the integration when $\boldsymbol{r} \cdot \boldsymbol{v} = 0$ must also be known precisely, so that $\theta_\oplus$ at t_{f_0} will be exactly the position of the Earth at the end of the forward transfer from LEO, or in other words, the value of $\theta_\oplus$ at $t = 0$ at the injection point, which is obtained internally by moving the Earth backward in time during the backward integration from t_{f_0}, corresponds to its exact location. This is needed because the inertial quantities are related to the actual position of the Earth along its orbit around the sun. These iterations on the t_{f_0} time have been automated by the iterator in which an outside loop updates t_{f_0} each time before another search is carried out until t is very near zero. A series of runs is generated for $h_T = 185$ km, but with different ω_T values. There is clearly a range of values for ω_T, for which the transfer solution is feasible because the injection into the long transfer orbit at LEO must take place on the appropriate side of the Earth to move the spacecraft in the direction of the L_1 point. The results of the converged runs are shown in Tables 1 and 2 for the range of ω_T values spanning the 40–168 deg range. All cases use the same value of $t_M = 8.91379 \times 10^6$ s. The maneuver ΔV at the halo point varies from 226 m/s for $\omega_T = 40$ to the minimum 32.248 m/s for $\omega_T = 168$ deg. Furthermore, as this minimum solution is approached, the convergence process slows down dramatically requiring tens of iterations to drive t to zero. The injection ΔV_{inj} decreases as ω_T is increased, and it reaches its minimum where the maneuver ΔV at the halo point is also at its minimum. The transfer times also vary from a low value of 95.55 days to about 108.620 for the $\omega_T = 168$ deg case showing that the longer trajectory results in the lower ΔV case. The inclination and right ascension of the ascending node of the departure hyperbola are left uncontrolled with i_0 steadily decreasing from 24.90 deg at $\omega_T = 40$ to 10.46 deg at $\omega_T = 110$ deg and then increasing back to 23.69 deg at $\omega_T = 168$ deg. The node, on the other hand, steadily decreases from 77.66 deg at $\omega_T = 40$ to -18.10 deg at $\omega_T = 168$ deg. The achieved values of the desired h_T and ω_T target values are also listed as h_0, ω_0, showing how h_T is often matched to within a meter and ω_T matched to within a hundreth of a degree. Finally, $\boldsymbol{r} \cdot \boldsymbol{v}$ at the endpoint or the injection point at LEO is also tabulated for all of the cases showing effectively that the flight-path angle is essentially equal to zero indicating perigee as desired. The three-parameter search problem, in which $\Delta\dot{x}$, $\Delta\dot{y}$, and $\Delta\dot{z}$ are iterated starting from guessed values, to match three parameters at the LEO injection point, namely, h_T, ω_T, and i_T, is carried out with the same outside loop that also drives the end time to zero.

When $\omega_T = 40$ deg, $h_T = 185$ km, and $i_T = 25$ deg, as well as $t_M = 8.91379 \times 10^6$ s, and when the initial guesses $\Delta\dot{x} = -88$ m/s, $\Delta\dot{y} = -62$ m/s, and $\Delta\dot{z} = 15$ m/s are used, a converged trajectory is obtained in a single run, after several iterations with solution given by $\Delta\dot{x} = -187.802593$ m/s, $\Delta\dot{y} = -133.461053$ m/s,

Table 1 Converged maneuver components for h_T = 185 km

ω_T (Target), deg	$\Delta\dot{x}$ Initial guess, m/s	$\Delta\dot{y}$ Initial guess, m/s	$\Delta\dot{x}$ Solution, m/s	$\Delta\dot{y}$ Solution, m/s	ΔV, m/s	ΔV_{inj}, km/s
40	−125.000	−90.000	−184.385117	−131.298283	226.356158	3.26884142
50	−99.000	−71.000	−125.2345000	−90.8327579	154.707046	3.26658090
60	−85.000	−60.000	−99.3186215	−71.3215344	122.274077	3.26568423
70	−75.000	−52.000	−84.5669543	−59.7842289	103.565070	3.26520446
80	−67.000	−46.000	−74.6906975	−51.9151476	90.9608864	3.26489738
90	−60.000	−40.000	−67.2880568	−45.9597108	81.4860577	3.26467542
100	−40.000	−20.000	−61.2712273	−41.0973539	73.7777459	3.26450068
110	−40.000	−20.000	−56.0215797	−36.8521282	67.0559225	3.26435271
120	−40.000	−20.000	−51.1648261	−32.9367818	60.8495770	3.26422000
130	−40.000	−20.000	−46.4281668	−29.1490894	54.8201065	3.26409493
140	−40.000	−20.000	−41.5916116	−25.3459599	48.7060555	3.26397246
150	−40.000	−20.000	−36.4898408	−21.4779411	42.3415923	3.26385071
160	−40.000	−20.000	−31.1953200	−17.8530431	35.9427203	3.26373776
165	−31.000	−17.000	−28.8040855	−16.6251416	33.2576409	3.26369760
166	−28.000	−16.000	−28.4020693	−16.4989170	32.8464884	3.26369276
167	−28.400	−16.500	28.0434595	−16.4344249	32.5042450	3.26368957
168	−28.000	−16.400	−27.7397765	−16.4455180	32.2482599	3.26368836

Table 2 Initial orbit parameters and transfer time for h_T = 185 km

ω_T, deg	Transfer time guess, s	Integration end time, s	Transfer time, s (days)	$\boldsymbol{r}\cdot\boldsymbol{v}$, km^2/s	h_0, km	ω_0, deg	i_0, deg	Ω_0, deg
40	8.3×10^6	−0.62553	8.40545361×10^6 (97.2853427)	0.31637×10^{-9}	184.990474	40.0104159	24.9071207	77.6684214
50	8.3×10^6	0.07468	8.25578563×10^6 (95.5530744)	-0.24124×10^{-10}	185.015334	49.9827805	18.3970545	74.6428431
60	8.3×10^6	−0.17276	8.28011686×10^6 (95.8346859)	0.29801×10^{-9}	185.001548	59.9974792	14.8523045	68.4316806
70	8.4×10^6	0.08560	8.32990491×10^6 (96.4109365)	-0.15906×10^{-9}	185.003108	69.9944290	12.7779275	60.9186467
80	8.5×10^6	0.33486	8.38304460×10^6 (97.0259791)	-0.59068×10^{-10}	185.002362	79.9878452	11.5240708	52.7711012
90	8.5×10^6	0.03128	8.43636180×10^6 (97.6430764)	-0.48067×10^{-11}	184.999861	89.9998019	10.7971490	44.2716311
100	8.8×10^6	−0.43460	8.49045741×10^6 (98.2691830)	-0.23696×10^{-9}	184.996928	99.9972092	10.4617521	35.6096975
110	8.8×10^6	0.08302	8.54755191×10^6 (98.9299990)	-0.23143×10^{-9}	184.998807	109.999052	10.4601518	26.8735798
120	8.8×10^6	−0.02056	8.61078070×10^6 (99.6618136)	-0.15461×10^{-9}	184.998643	119.999166	10.7926547	18.1532924
130	8.8×10^6	0.05765	8.68501229×10^6 (100.520976)	0.15348×10^{-9}	184.998542	129.999228	11.5164021	9.53681062
140	8.8×10^6	0.08610	8.77851621×10^6 (101.603197)	-0.63460×10^{-10}	184.998494	139.999260	12.7721443	1.14665011
150	8.8×10^6	0.08004	8.90732035×10^6 (103.093986)	0.13575×10^{-9}	184.998508	149.999299	14.8633709	−6.80656875
160	8.8×10^6	0.00016	9.10800105×10^6 (105.416679)	-0.24380×10^{-10}	185.000242	160.000206	18.4909135	−13.8733209
165	9.1×10^6	0.11258	9.26191539×10^6 (107.198095)	-0.16009×10^{-9}	184.998430	164.999488	21.3786509	−16.7524563
166	9.2×10^6	−0.41429	9.29973633×10^6 (107.635837)	-0.70526×10^{-10}	184.998751	165.999587	22.0921647	−17.2429860
167	9.3×10^6	−0.51324	9.34056308×10^6 (108.108369)	-0.54000×10^{-9}	184.998444	166.999568	22.8626882	−17.6967755
168	9.34×10^6	−0.24704	9.38478804×10^6 (108.620232)	-0.61129×10^{-9}	184.998972	167.999829	23.6970997	−18.1092916

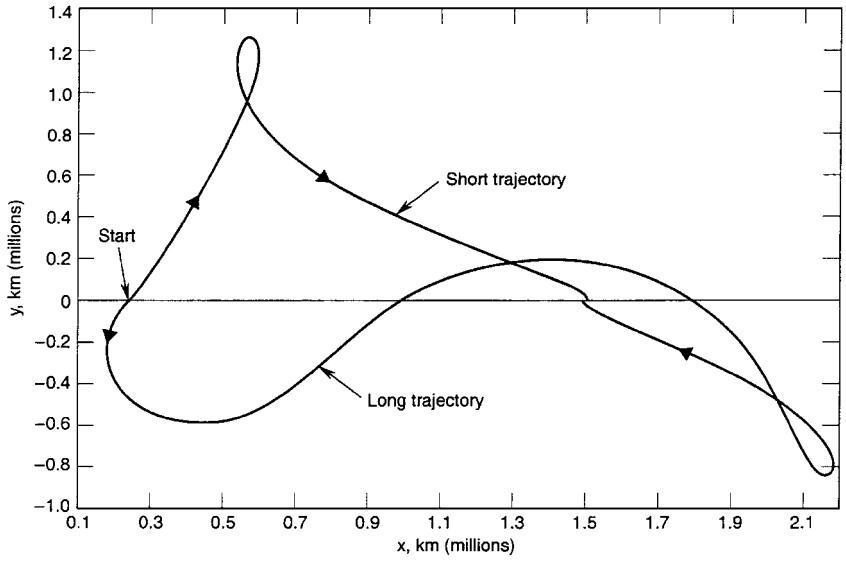

Fig. 3 Traces of x–y of short and long trajectories for target (i_T = 25 deg, ω_T = 40 deg, and h_T = 185 km).

$\Delta\dot{z} = -0.397062$ m/s, yielding $\Delta V = 230.394931$ m/s, and terminating at $t = -0.397853$ s with, $a_0 = -0.440768135\times10^6$ km, $e_0 = 1.01489020, \Omega_0 = 77.2787483$ deg, and $\theta_0^* = 360.000000$ deg, with corresponding $\Delta V_{\text{inj}} = 3.26898298$ km/s. The achieved target parameters are $i_0 = 24.9992903$ deg, $h_0 = 184.987469$ km, and $\omega_0 = 39.9996966$ deg, with $\gamma_0 = 0.000000000$ deg, $\boldsymbol{r}\cdot\boldsymbol{v} = -0.471096\times10^{-9}$ km^2/s, and a transfer time $t_f = 97.4576876$ days. Figure 3 shows the x–y trace of this transfer, labeled short trajectory, integrated backward from the x–z crossing point of the halo orbit to the LEO intersection orbit. Another type of transfer is generated by using a deliberately large initial guess with solution given by $\Delta\dot{x} = 157.021207$ m/s, $\Delta\dot{y} = 534.394283$ m/s, and $\Delta\dot{z} = 327.930490$ m/s, for a maneuver ΔV of 646.352315 m/s and terminating at $t = 0.99404$ s with $a_0 = -0.455736625\times10^6$ km, $e_0 = 1.01440100$, $\Omega_0 = -109.948160$ deg, $\omega_0 = 40.0034246$ deg, $\theta_0^* = 0.2321\times10^{-12}$ deg, $i_0 = 25.0059611$ deg, $h_0 = 184.924417$ km, with $\boldsymbol{r}\cdot\boldsymbol{v} = 0.14808\times10^{-9}$ km^2/s, $\gamma_0 = 0.000000000$ deg, and transfer time $t_f = 141.076744$ days. The injection ΔV_{inj} needed to depart the LEO orbit on this hyperbolic trajectory is equal to $\Delta V_{\text{inj}} = 3.26764037$ km/s. This

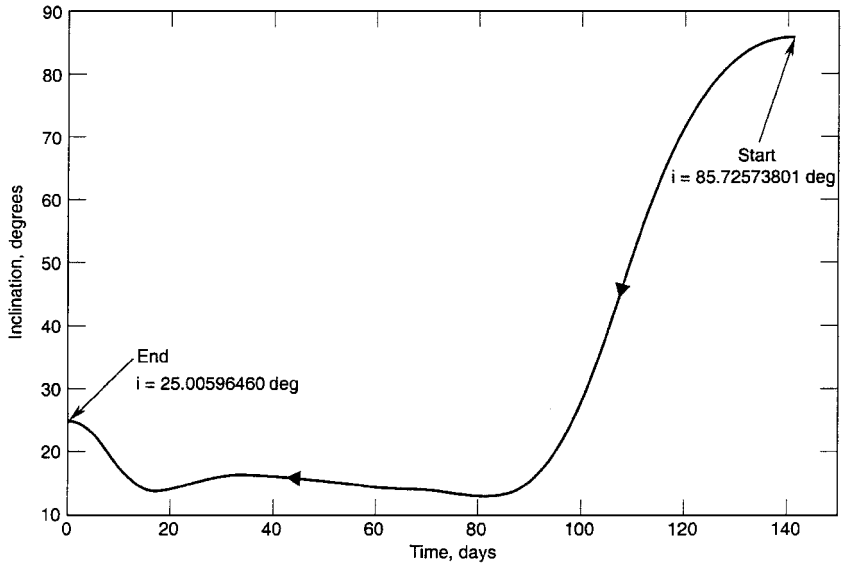

Fig. 4 Evolution of inclination for long trajectory integrated backward.

backward-integrated path labeled long trajectory, is also shown in Fig. 3. The injection point is about 180 deg away from that of the short trajectory, showing how the hyperbolic orbit moves the spacecraft away from the sun with a loop taking place at about 2.1×10^6 km from the L_1 point, as opposed to the short trajectory loop, which takes place at 0.5×10^6 km from L_1 in the positive y region. The ΔV needed at insertion is much higher than for the short trajectory case, the flight-path angle γ has four zeros as the trajectory moves in the sun–Earth system. The altitude history shows a close approach of the Earth near the midpoint of the trajectory at about 200,000 km, well inside the lunar orbit.

The inclination is shown in Fig. 4, showing how the sun's perturbation affects the initial low inclination at departure from LEO, rotating the orbit plane beyond the 85-deg mark. The spacecraft orbit plane precesses backward by about 150 deg as the vehicle reaches its halo point destination. The evolution of the Earth-centered inertial velocity shows a hump near the midpoint of the trajectory where the velocity peaks at about 2 km/s before dropping down, corresponding to the near-Earth flyby required by this long trajectory. As for the two-parameter search cases of Tables 1 and 2, similar tables can be produced for a fixed i_T value and for varying ω_T values to determine both the feasible ω_T range for which transfers are feasible and also for selecting that particular value of ω_T that results in the lower halo insertion ΔV. When this search is carried out for various values of i_T, the ideal initial i_T and ω_T pair can be determined for a minimum-ΔV solution and the feasible i_T and ω_T ranges established. This whole search space must then involve the entire halo orbit to establish the family of solution sets that provide the lower insertion ΔV.

Conclusions

LEO to L_1-centered halo orbit transfers with meter accuracy are generated after regularizing the original singular differential equations of motion in terms of rotating coordinates centered at the convenient L_1 Lagrange libration point of the sun–Earth system using the classic restricted circular three-body model. Various aspects of the integration termination criteria as well as the iterations needed for a precise computation of the transfer time using the backward integration scheme are also discussed leading to the accurate determination of the required orbit plane orientation for departure from LEO. The transfer time from LEO to the halo orbit, as well as the injection velocity change needed to escape Earth, and the corresponding right ascension of the ascending node at injection are all byproducts of the search procedure that solves for the three components of the velocity change at the halo orbit location of interest to meet through backward integration a desired target altitude, inclination, and perigee location at the LEO injection point. This analysis can be extended to the more exacting restricted elliptic three-body model in which the Earth and the sun move in elliptic orbits around their common moving barycenter and with minor modifications to transfers to the L_2 point as well as to other binary systems such as the Earth–moon system.

Acknowledgment

This work was supported by the U.S. Air Force Space and Missile Systems Center under Contract F04701-93-C-0094.

References

[1]Farquhar, R. W., "The Control and Use of Libration-Point Satellites," NASA TR R-346, 1970.

[2]Farquhar, R. W., Muhonen, D. P., and Richardson, D. L., "Mission Design for a Halo Orbiter of the Earth," *Journal of Spacecraft*, Vol. 14, No. 3, 1977, pp. 170–177.

[3]Farquhar, R. W., Muhonen, D. P., Newman, C. R., and Heuberger, H. S., "Trajectories and Orbital Maneuvers for the First Libration-Point Satellite," *Journal of Guidance and Control*, Vol. 3, No. 6, 1980, pp. 549–554.

[4]Farquhar, R. W., "Halo-Orbit and Lunar Swingby Missions of the 1990's," *Acta Astronautica*, Vol. 24, 1991, pp. 227–234.

[5]Howell, K. C., and Breakwell, J. V., "Almost Rectilinear Halo Orbits," *Celestial Mechanics*, Vol. 32, 1984, pp. 24–52.

[6]Mains, D. L., "Transfer Trajectories from Earth Parking Orbits to L_1 Halo Orbits," M.S. Thesis, Dept. of Aeronautics and Astronautics, Purdue Univ., Lafayette, IN, May 1993.

[7]Kustaanheimo, P., "Spinor Regularization of the Kepler Motion," *Annales Universitatis Turkuensis Series AI*, Vol. 73, 1964, pp. 1–7.

[8]Kustaanheimo, P., and Stiefel, E., "Perturbation Theory of Kepler Motion Based on Spinor Regularization," *Journal für Mathematik*, Vol. 218, 1965, pp. 204–219.

[9]Levi-Civita, T., "Sur la Résolution Qualitative du Problème Restreint des Trois Corps," *Operemathematiche*, Vol. 2, 1956, pp. 99–144.

[10]Stiefel, E. L., and Scheifele, G., *Linear and Regular Celestial Mechanics*, Springer-Verlag, New York, 1971.

[11]Press, W. H., Flannery, B. P., Teukolsky, S. A., and Vetterling, W. T., *Numerical Recipes (Fortran)*, Cambridge Univ. Press, Cambridge, England, U.K., 1989.

[12]Kahaner, D., Moler, C., and Nash, S., *Numerical Methods and Software*, Prentice–Hall, Englewood Cliffs, NJ, 1989.